A familial missense variant in the Alzheimer's Disease gene *SORL1* impairs its maturation and endosomal sorting.

Elnaz Fazeli[1], Daniel D. Child[2], Stephanie A. Bucks[3], Miki Stovarsky[4], Gabrielle Edwards[3], Shannon E. Rose[2], Chang-En Yu[4,6], Caitlin Latimer[2], Yu Kitago[5], Thomas Bird[3,4,6], Suman Jayadev[3*], Olav M. Andersen[1*], and Jessica E. Young[2*]

***Co-corresponding authors**

[1] Department of Biomedicine, Aarhus University, Høegh-Guldbergs Gade 10, DK8000 AarhusC, Denmark

[2]Department of Laboratory Medicine and Pathology, University of Washington, Seattle Washington USA

[3]Department of Neurology, University of Washington, Seattle Washington USA

[4]Department of Medicine, Division of Medical Genetics University of Washington, Seattle Washington USA

[5]Ann Romney Center for Neurologic Diseases, Harvard Medical School and Brigham and Women's Hospital, Boston, MA 02115

[6]Geriatric Research Education and Clinical Center (GRECC), Veterans Administration Health Care System

Correspondence to: jeyoung@uw.edu, sumie@uw.edu, o.andersen@biomed.au.dk

Abstract

The *SORL1* gene has recently emerged as a strong Alzheimer's Disease (AD) risk gene. Over 500 different variants have been identified in the gene and the contribution of individual variants to AD development and progression is still largely unknown. Here, we describe a family consisting of 2 parents and 5 offspring. Both parents were affected with dementia and one had confirmed AD pathology with an age of onset >75 years. All offspring were affected with AD with ages at onset ranging from 53yrs-74yrs. DNA was available from the parent with confirmed AD and 5 offspring. We identified a coding variant, p.(Arg953Cys), in *SORL1* in 5 of 6 individuals affected by AD. Notably, variant carriers had severe AD pathology, and the *SORL1* variant segregated with

TDP-43 pathology (LATE-NC). We further characterized this variant and show that this Arginine substitution occurs at a critical position in the YWTD-domain of the *SORL1* translation product, SORL1. Functional studies further show that the p.R953C variant leads to retention of the SORL1 protein in the endoplasmic reticulum which leads to decreased maturation and shedding of the receptor and prevents its normal endosomal trafficking. Together, our analysis suggests that p.R953C is a pathogenic variant of *SORL1* and sheds light on mechanisms of how missense *SORL1* variants may lead to AD.

Running Title: Pathogenic *SORL1* variant impairs sorting

Keywords: *SORL1*; Alzheimer's disease; YWTD-domain; pathogenic variant; TDP-43

Introduction

Alzheimer Disease (AD) is the most common cause of dementia worldwide. The etiology of AD remains elusive, slowing development of disease modifying therapies. Pathogenic variants in *PSEN1*, *PSEN2* and *APP* are associated with autosomal dominantly inherited early-onset AD (ADAD), although those families are rare and make up only a very small fraction of all AD. Nevertheless, knowledge gained from studying ADAD has been valuable to our understanding of the clinical, pathological and mechanistic features of AD more broadly. Late onset AD also has a genetic component and is known to be highly heritable, estimated at 60-80%[33] and heritability can vary with age[9]. Genome wide association studies (GWAS) as well as genome and exome sequencing studies have revealed the complexity of biological processes contributing to AD risk and progression[70]. Given that families with AD likely harbor at least one AD genetic risk factor, they can provide important insight into genetic risk and disease pathogenesis.

The Sortilin-like receptor, *SORL1,* (protein: SORL1/SORLA) was originally identified as a member of the LDL receptor family, and the SORL1 protein is now classified as one of five mammalian sorting receptors called VPS10p receptors[31, 32, 72-74]. SORL1 functions as an endosomal receptor to assist cargo sorting out of the endosome to either the cell surface via the recycling pathway or to the trans-Golgi network (TGN) via the retrograde pathway[21, 24, 34, 51, 65]. For sorting of AD-related cargo, including Amyloid-β peptide (Aβ) and APP, SORL1 directly interacts with the multi-sorting complex retromer, itself highly implicated in endo-lysosomal health and neurodegeneration[18, 22, 57].

Through both candidate gene studies and GWAS, *SORL1* was found to be a strong genetic risk factor for AD[42, 43, 58, 59]. Exome-sequencing studies have shown that rare loss-of-function S*ORL1* alleles, leading to haploinsufficiency, have been associated with highly penetrant AD[25, 26, 55, 56, 71], although the full breadth and contribution of *SORL1* variants in AD is not fully defined. A large number (>500) of *SORL1* variants have been identified in patient populations with AD, but with variable levels of evidence for pathogenicity. Recently, two missense variants have been associated with autosomal dominant AD: p.(Asp1545Val) (Bjarnadottir et al., Manuscript in preparation) and p.(Tyr1816Cys)[35]. In case of the p.(Tyr1816Cys) we showed how this mutation has only minor impact on the intracellular localization per se, but strongly decreased receptor dimerization in endosomes and retromer-dependent recycling to the cell surface[35]. Reported *SORL1* variants span the length of the gene and functional domains, and how different pathogenic variants impair the overall functions of SORL1 as an endosomal sorting receptor is not yet clear. It has been suggested that SORL1 maturation, which is a distinct change in some of the *N*-glycans attached to the luminal SORL1 domain[14], is decreased for some *SORL1* missense variants[50, 60]. Defining the biochemical consequences of pathogenic *SORL1* missense variants can shed light on mechanisms of disease involving SORL1 and other components of the endo-lysosomal network (ELN).

We present here a family with early and late onset AD in two generations. Genetic testing confirmed a novel *SORL1* variant, c.2857C>T p.Arg953Cys (R953C; NM_003105.5) which affects a residue in one of the repeats in the YWTD-domain, in 6 out of 7 affected individuals tested. Neuropathological studies demonstrated severe AD pathology, including cerebellar amyloid plaques, cortical neurofibrillary tangles, and TDP-43 deposition despite a young age of onset in most carriers of the *SORL1* R953C variant. One individual, I-2, was affected with AD but did not carry the SORL1 variant and did not show TDP-43 deposition. To further characterize this genetic variant, we turned to a previously described disease-mutation domain-mapping approach that relies on identified pathogenic variants in homologous proteins including members of the LDLR family[8], to predict pathogenicity based on the domain position at which the variant occurs in SORL1. We next generated a plasmid containing the p.R953C variant and transfected it into HEK293 and N2a cells. Our *in vitro* studies suggest reduced SORL1 maturation and impaired endosomal localization, confirming a functional consequence of the missense variant. The

influence of the variant on SORL1 cellular localization may lead to impairment of endosomal sorting and have pathogenic effects. This study adds to the growing body of literature supporting a role for *SORL1* variants that may contribute to the missing AD heritability.

Methods

Study Participants

The family was ascertained by the University of Washington Alzheimer Disease Research Center. The study was approved by the UW Institutional Review Board (IRB) and all participants provided written consents.

Genetic Studies

Genetic analysis was performed by the Northwest Clinical Genomics Laboratory (NCGL), a CLIA certified laboratory at the University of Washington. Samples underwent next-generation exome sequencing and analysis. Libraries were constructed according to the NCGL protocol. The KAPA Hyper Prep DNA library kit (KAPA Biosystems, Wilmington, MA, USA) was used to prepare the libraries, which were subsequently enriched using an in-house, optimized xGen Exome Research Panel v1.0 (Integrated DNA Technologies, Coralville, IA, USA). Paired-end sequencing of the exome-enriched libraries was performed on a HiSeq 4000 instrument (Illumina, San Diego, CA, USA). Greater than 99% of the coding regions and canonical splice sites were sequenced to a read coverage of at least 20X or greater. The average mean depth of coverage was 144 reads. Resulting sequences were aligned to the human genome reference (hg19) using the Burrows-Wheeler Aligner (BWA)[46]. Variants were identified using the Genome Analysis Toolkit (GATK)[19, 49]and were annotated using the SnpEff annotation tool[15] in combination with various population databases and variant impact scoring tools. Individual II-5 was initially screened with a 39-gene dementia panel which included: *APP*, *ARSA, APOE, ATP13A2, CHCHD10, CHMP2B, CSF1R, DNMT1, EIF2B1, EIF2B2, EIF2B3, EIF2B4, EIF2B5, FUS, GALC, GRN, HEXA, ITM2B, LMNB1, MAPT, NOTCH3, NPC1, NPC2, OPA1, PDGFB, PDGFRB, PLP1, PRNP, PSEN1, PSEN2, SLC20A2, SLC25A12, SORL1, TARDBP, TBK1, TBP, TREM2, TYROBP, VCP* which identified the *SORL1* p.R953C variant. Whole exome sequencing was then performed on II-1, II-2, II-4 and II-5 to evaluate for any other candidate variants and to investigate which variants segregated with the phenotype. Shared variants were filtered based on population data and variants

with an allele frequency greater than 0.001 in ExAC were excluded from further analysis. Variants were manually evaluated through literature searches in PubMed. II-1, II-2, II-4 were also found to carry the *SORL1* p.R953C variant via exome sequencing. No other variants associated with dementing disorders were identified. II-3 was later found to carry the variant using Sanger sequencing.

APOE genotyping:

APOE genotyping was performed as previously published[44]. Briefly, genomic DNA was amplified in a 9700 Gene Amp PCR System (Applied Biosystems) using primers that amplify *APOE* gene's exon 4. This PCR amplicon includes both the codon 112 (ε2/ε3 vs. ε4) and codon 158 (ε2 vs. ε3/ε4) polymorphic sites.

Taqman assay: SNPs rs429358 (ε2/ε3 vs. ε4) and rs7412 (ε2 vs. ε3/ε4) were genotyped using assay C_3084793_20 and assay C_904973_10 (Thermo Fisher), respectively. All reactions were carried out in a 9700 Gene Amp PCR System with a profile of 50°C for 5 minutes; 95°C for 5 minutes; 50 cycles of 95°C for 15 seconds, and 60°C for 1 minute.

Sanger sequencing: The PCR reaction/amplicon (1 µl) was used in BigDye sequencing reaction (Thermo Fisher) with a final volume of 10 µl. All reactions were carried out in a 9700 Gene Amp PCR System with a profile of 94°C for 1 minute; 35 cycles of 94°C for 30 seconds, 55°C for 10 seconds, and 60°C for 4 minutes; and a final extension of 60°C for 5 minutes. The PCR generated sequencing products were further purified using EDTA/ethanol precipitation and then subjected to DNA sequencing run using SeqStudio (Thermo Fisher). The sequencing data (electropherograms) were transferred and uploaded onto the Sequencher program (Genecodes) for sequence alignment.

Primer sequences:

APOE_Ex4_F: 5' TCGGAACTGGAGGAACAACT 3'

APOE_Ex4_R: 5' GCTCGAACCAGCTCTTGAGG 3'

SORL1 genotyping

SORL1 variant genotyping was performed on I-2, II-2, II-3, and III-6. Genomic DNA was amplified with Phusion Flash (Thermo Fisher) on a C1000 Touch Thermo cycler (BioRad) using primers that amplify exon 20 in *SORL1*. Cycle conditions: 98°C for 10s; 98°C for 1s, 65°C for 5s, 72°C for 10s X25 cycles; 72°C for 1 min. Cleaned PCR reactions were sent for Sanger sequencing

using GeneWiz (Azenta Life Sciences). Sequences were examined manually using 4 Peaks software.

Primer sequences:

SORL1 F: 5' GCCTGGGATTTATCGGAGCA 3'

SORL1 R: 5' TGGCATCCCTCCATAGGCT 3'

Neuropathology

Consent for autopsy was obtained from the donor or from the legal next of kin, according to the protocols approved by the UW Institutional Review Board. At the time of autopsy, the brain was removed in the usual fashion. For patients I-2, II-2, II-3 and II-4, the left halves were coronally sectioned and samples were frozen for possible biochemical studies and the right halves were fixed in formalin. For patients II-1 and II-5, the entire brain was fixed in formalin. After fixation, the cerebrum was sectioned coronally, the brainstem was sectioned axially, and the cerebellum was sectioned sagittally.

Representative sections for histology were selected and evaluated according to National Institute of Aging-Alzheimer's Association (NIA-AA) guidelines[52]. A microtome was used to cut 4 μm-thick tissue sections from formalin-fixed, paraffin-embedded tissue blocks. Hematoxylin and eosin (H&E), Luxol fast blue (LFB), and Bielschowsky silver-stained slides were prepared. Using previously optimized conditions, immunohistochemistry was performed using a Leica Bond III Fully Automated IHC and ISH Staining System (Leica Biosystems, Wetzlar, Germany). The sections were immunostained with mouse monoclonal antibody against paired helical filament tau (AT8, 1:1,000 dilution) (Pierce Technology, Waltham, MA), mouse monoclonal against β-amyloid (6E10, 1:5,000) (Covance, Princeton, NJ), rat monoclonal against phosphorylated TDP-43 (ser409/ser410, 1:1,000) (Millipore, Burlington, MA), and mouse monoclonal against α-synuclein (LB509, 1:500) (Invitrogen, Carlsbad, CA). Appropriate positive and negative controls were included with each antibody and each run.

Site-directed Mutagenesis

The R953C variant was inserted in *SORL1* pcDNA3.1 and *SORL1*-GFP pcDNA3.1 using site directed mutagenesis kit (QuikChange #200521) according to manufacturers' instruction with the

following pair of primers: 5- gga tca cgt tca gtg gcc agc agt gct ctg tca ttc tgg aca acc tcc-3 and 5-gga ggt tgt cca gaa tga cag agc act gct ggc cac tga acg tga tcc-3.

Cell transfection and western blotting

Approximately $5x10^5$ HEK293 and N2a cells were seeded on 6-well plates and transiently transfected with expression constructs for *SORL1*-WT or *SORL1*-R953C, using Fugene 6 Transfection Reagent kit (Promega) according to manufacturers' instructions. 48 hours post transfection, cell medium was changed to serum free conditional medium and after 48 hours, cells and media were harvested. Cells were lysed using lysis buffer (Tris 20mM, EDTA 10mM, TritonX 1%, NP40 1%). Media samples (30ml) and lysate samples(20ug) were mixed with NuPAGE LDS sample buffer (Invitrogen, #2463558) supplemented with β-Mercaptoethanol (Sigma) and separated on SDS-PAGE using 4–12% NuPAGE Bis-Tris gels (Thermo). Proteins were then transferred to nitrocellulose membranes (Thermo) and incubated for 1h at room temperature in Blocking buffer (Tris-Base 0.25M, NaCl 2.5M, skimmed milk powder 2%, tween-20 2%). Next, membranes were incubated overnight at 4°C with LR11 antibody 1:1,000 (BDBiosciences # 612633) to detect SORL1 and Beta actin 1:2,000 (Sigma #A5441) as loading control, followed by three washes for 5 minutes in washing buffer ($CaCl_2$ 0.2 mM, $MgCl_2$ 0.1 mM, HEPES 1 mM, NaCl 14 mM, skimmed milk powder 0.2%, Tween 20 0.05%) and 1 hour incubation with HRP-conjugated secondary antibody (1:1,500, Dako, #P0260) for 1 hour at room temperature. Membranes were washed 5 times for 5 minutes, incubated with FEMTO detection reagent (Thermo #34095) and visualized by iBright1500 scanner. Quantification was performed by densitometric analysis in ImageJ and data were plotted in Graphpad Prism 9.5.0.

Flow cytometry

Cell surface and total receptor level were analyzed by flow cytometry in live, transfected HEK293 and N2a cells. Briefly, HEK293 and N2a cells were transiently transfected with either *SORL1*-GFP-WT or *SORL1*-GFP-R953C plasmids. Twenty-four hours after transfection, cells were collected by trypsinization, pelleted, and resuspended in phosphate-buffered saline (PBS pH 7.4). After 15min incubation in blocking buffer (PBS pH 7.4 ,0.5% BSA), cells were immunostained at 4°C with rabbit anti-soluble-SORL1 primary antibody followed by washing two times with PBS pH 7.4 and 30min incubation with Alexa-flour 647 secondary antibody in the absence of detergent

followed by 3 times washing and finally resuspension in FACS buffer (PBS pH 7.4, 2% FBS, 1% Glucose). Cells were analyzed by NovoCyte 3000 flow cytometer equipped with three lasers and 13 fluorescence detectors (Agilent, Santa Clara, CA). GFP and Alexa Flour 647 fluorophores were excited by the 488 and 640 nm lasers, respectively. Results were analyzed using FlowJo™ v10.8.1 Software (BD Life Sciences).

Immunocytochemistry and Confocal Microscopy

Approximately $5x10^4$ HEK293 cells were seeded on poly-L-lysine coated glass coverslips and transfected with expression constructs for *SORL1*-WT or *SORL1*-R953C using Fugene 6 Transfection Reagent kit (Promega). 24h post-transfection, cells were fixed with PFA 4% for 10 minutes at room temperature, followed by a wash in PBS pH 7.4. Coverslips were washed twice in PBS with 0.1% Triton-X 100 (for intracellular staining) or only PBS (for membrane staining) and later blocked for 30 minutes at room temperature in blocking buffer (PBS, FBS 10%). Cells were then incubated overnight at 4°C with pAb_5387 (a polyclonal rabbit serum generated for the entire SORL1 ectodomain[31]) antibody alone or with an antibody against markers specific for each intracellular compartment (EEA1 for early endosomes, TFR for recycling endosomes, and Calnexin for ER). Next, cells were washed in PBS with or without Triton-X 0.1 % and incubated in Alexa Flour secondary antibodies (Invitrogen, 1:500) for 1 hour at room temperature. After washing once in PBS, cells were stained with Höechst (Abcam, 1:50,000) for 10 minutes at room temperature. The coverslips were then mounted on glass slides using DAKO fluorescence mounting medium (Agilent) and were imaged using Zeiss LSM800 confocal microscope. Colocalization was quantified using the JACOP plugin in ImageJ software and presented as Mander's correlation coefficient. Graphing and statistical analysis of the data were performed with GraphPad Prism 9.5.0. Antibodies used were as follows: rabbit polyclonal anti-SORL1 (pAb_5387; Aarhus University) 1:300, mouse monoclonal anti-SORL1 (mAb_AG4; Aarhus University) 1:100, anti EEA1(#610457 BDBiosciences) 1:100, anti TFR 1:100(# A-11130 Invitrogen), anti-Calnexin (1:100) (#610523 BDBiosciences).

Statistical analysis.

The data are represented as the mean ± s.d. The 'n' numbers represent the number of biological replicates in each experiment, while for imaging studies 'n' represents the total number of cells

analyzed. Data was analyzed using parametric two-tailed paired (WB analysis and flow cytometry) or unpaired (immunostaining) t-tests. A P-value of less than 0.05 is considered statistically significant. All statistical analysis was completed using GraphPad Prism 9.5.0 software.

Data Availability

The authors confirm that the data supporting the findings of this study are available within the article and/or its supplementary material or available from a corresponding author upon reasonable request.

Results

Clinical Description

Three generations (**Figure 1**) of the study family are presented here. Clinical features are reported in **Table 1**. Both parents (I-1 and I-2) developed late onset dementia and I-1 also demonstrated parkinsonism and aggressive behavior. Of the 5 individuals in the II generation sibship, 4 were clinically diagnosed with AD, with a range of age of onset from 51 years to 73 years. II-3 was reported to carry a clinical diagnosis of dementia prior to death and had age of onset 74 yrs. II-4 and II-5, identical twins, developed early onset AD at age 57 years and 51 years, respectively. II-5 developed aphasia and apraxia in addition to memory loss. III-6, daughter of II-2, developed progressive spasticity at age 44. She has also developed evidence of executive dysfunction determined by neuropsychiatric evaluation at age 45 and again on repeat testing at age 46 without progression. She has not shown any lower motor neuron findings or any other neurological signs. MRI brain did not show atrophy or other abnormality (data not shown).

Neuropathology

Individuals I-2, II-1, II-2, II-3, II-4, and II-5 were evaluated at autopsy, and findings are summarized in **Table 2**. Brain weight in all cases except II-1 was below the 10^{th} percentile for age and sex[10]. Atherosclerosis was present in all cases, with plaques extending beyond the first branch point of at least one cerebral artery (defined here as moderate); in case II-4, atherosclerotic plaques were also visible on the external surface and thus graded as severe. No other abnormalities were observed grossly in any case.

Histopathology

All autopsy cases were evaluated by the standard NIA-AA protocol[30, 52]. β-amyloid plaques progressed to the midbrain in cases I-2 and II-1 (Thal phase 4 of 5), and extended to the cerebellum in cases II-2, II-3, II-4, and II-5 (Thal phase 5 of 5, **Figure 2a**). Tau tangles were present within the calcarine cortex/primary visual cortex in all cases (Braak and Braak stage VI of VI, **Figure 2b**). Cortical neuritic plaque density in all cases was frequent by Consortium to Establish a Registry for Alzheimer's Disease (CERAD) criteria (**Figure 2c**). The features in each case meet criteria for high Alzheimer's disease neuropathologic change (ADNC) by NIA-AA guidelines[52]. Additionally, all generation II cases had TDP-43 inclusions in the amygdala and hippocampus,

consistent with limbic-predominant age-related TDP-43 encephalopathy neuropathologic change (LATE-NC) stage 1 or 2 out of 3[53] (**Figure 2d**); TDP-43 inclusions were not seen in case I-2 (*SORL1* variant negative). Hippocampal sclerosis was also seen in cases II-2 and II-4. Varying stages of Lewy body disease (LBD) were also identified, with diffuse (neocortical) LBD diagnosed in II-1, limbic (transitional) LBD in II-2, and brainstem-predominant LBD in II-4 (**Figure 2e).** We present neuropathological findings of all subjects that underwent brain autopsy in **Figure 3.**

Genetic Findings

Due to early onset and family history of AD, subject II-5 underwent *PSEN1* and *APP* research genetic testing, which was negative in both genes. Years after the subject's passing, his genetic material was included in an early onset AD cohort evaluated by an exome panel of 39 neurodegeneration genes. II-5 was found to carry a *SORL1* missense variant: NM_003105.5 c.2857C>T p.Arg953Cys (R953C). The reported allele frequency of this variant in gnomAD for those of European (non-Finnish) ancestry is 1/113646. It has not been reported in other populations assessed. In silico predictions varied; Polyphen: probably damaging, SIFT: tolerated, REVEL: 0.805, CADD v1.3: 25.4, PrimateAI: 0.633. No other pathogenic or likely pathogenic variants were identified in the other 38 genes on the neurodegeneration panel. Next, we screened II-1, II-2, II-4, and II-5 by whole exome sequencing, which revealed that all four subjects carry the *SORL1* R953C variant and no other pathogenic variants known to be associated with dementia were identified. We re-confirmed the presence of the *SORL1* R953C in II-2 variant using Sanger sequencing. II-3 passed away during preparation of this manuscript. We performed Sanger sequencing and confirmed the presence of the *SORL1* R953C variant in II-3. Using Sanger sequencing, we found that I-2 did not carry the *SORL1* variant, and no DNA samples were available from I-1. III-6 was found to carry the *SORL1* variant using Sanger sequencing of dermal fibroblasts. All Sanger sequencing results are presented in **Supplemental Figure 1**. C9orf72 gene expansion testing was negative in generation II and III-6. I-2, all individuals in the II generation and III-6 have an APOE ε3/ε3 genotype.

Variant characterization

The arginine residue Arg953 is located at blade position 38 of the YWTD-domain repeated sequence, located within the fifth of six repeats that build the 6-bladed β-propeller domain of

SORL1 (**Figure 4a**). We previously undertook a detailed disease-mutation domain-mapping approach to identify the most pathogenic sequence positions for the SORL1 domains and their risk for developing AD[8]. From this analysis, YWTD-domain sequence position 38 was identified as a high-risk site when arginine substitution occurs, and we identified variant p.Arg953His, (p.R953H) in three early-onset AD patients corresponding to the same SORL1 amino acid. However, the p.R953C variant was not identified in this large exome-sequencing study[25]. From previous disease mapping work[8], we identified 5 pathogenic variants in homologous proteins corresponding to substitution of an arginine at the YWTD-domain sequence position 38, summarized in **Table 3**. We report variant classification by VarSome, a search engine that aggregates databases, including ClinVar, and annotates pathogenicity of variants using the ACMG/AMP guidelines[41].

Familial hypercholesterolemia (FH) is an autosomal dominant disorder with a prevalence of approximately 1 in 500 and most frequently caused by mutations in the gene for the low-density lipoprotein receptor (LDLR). The variant p.R595W^{LDLR} has been identified in patients with FH family history in cohorts from Belgium[20] and Taiwan[13] and considered an autosomal dominant variant.

Variants in another member of the LDLR gene family, LRP5, has been associated with a number of monogenic diseases, and different variants are often the cause of different clinical disorders. The p.R1188W^{LRP5} has been identified to segregate in a 40-member Dutch family with three generations of early- and late-onset cystogenesis inherited in an autosomal dominant fashion with Polycystic Liver Disease (PCLD). Cell-based studies to assess receptor activity confirmed significantly decreased activity of the mutated receptor compared to wild-type LRP5[16].

Osteoporosis-Pseudoglioma Syndrome (OPPG) is an autosomal recessive disorder and is caused by homozygous pathogenic variants in LRP5, due to the receptor function as a key regulator of bone metabolism through the Wnt signaling pathway. The biallelic presence of the pathogenic variant p.R494Q^{LRP5} has been identified as the cause of OPPG in families with homozygous carriers of the mutation[1, 3, 23]. Moreover, the p.R494W^{LRP5} that affects the same amino acid of LRP5 was identified as a potential pathogenic variant in a patient with Familial Exudative Vitreoretinopathy (FEVR), adding further support to the critical role of this amino acid to produce functional LRP5[47].

The variant p.R752G^{LRP5} was also identified as the cause of disease in a compound homozygous carrier for the FEVR autosomal recessive disorder [36]. Another variant that affects the same amino acid in LRP5; p.R752W^{LRP5} has been reported to associate with low bone mineral density in a female heterozygous carrier, and in combination with another pathogenic LRP5 variant (p.W79R that affects a YWTD-motif residue) in her son causes a severe case of compound heterozygous OPPG[4]. Moreover, the p.R752W^{LRP5} was identified as a potential pathogenic variant in a patient with FEVR when it was identified in a compound heterozygous carrier together with the pathogenic p.C1305Y variants in LRP5[27]. These studies add further support to the critical role of the arginine amino acid at domain position 38 to produce functional LRP5. A variant, p.R632H^{LRP4}, affects the homologous receptor LRP4. This variant is causal for sclerosteosis when present as heterozygous compound mutation together with another pathogenic variant in LRP4 (p.R1170Q). Cell based assays confirmed how both of these mutations in LRP4 reduced receptor activity, providing support of the important function of the arginine also within the YWTD-domain of LRP4[29]. We summarize these findings and literature in **Table 3**.

We recently prepared a three-dimensional model of the SORL1 ectodomain including its YWTD-domain using the AlphaFold2 algorithm[34]. Here, we used this model to investigate the functional role of the arginine side chain (**Figure 4b, d**). From this model it is observed that the positively charged amino group makes ionic contacts with the side chain of the glutamic acid residue at blade-sequence position 28 (E944 of SORL1) serving to position the long arginine side chain in place to make further hydrogen bonds to two backbone carbonyls in the preceding loop between blades (**Figure 4d**), thereby strongly contributing to the folding and the stability of the entire six-bladed β-propeller domain. Interestingly, in four of the five blade-sequences containing the identified disease variants, a glutamic acid is similarly located at blade-sequence position 28 (**Figure 4c**).

Inspection of a larger alignment of YWTD-repeat sequences revealed that for most blade-sequences, a similar pattern is observed: when an arginine occupies blade-sequence at position 38, then a glutamate resides at blade-sequence position 28[8], suggesting this pair of residues may generally be important for the folding of YWTD-domains.

The crystal structures of the YWTD-domains have previously been solved for LDLR[61] and LPR4[75] including R595^{LDLR} and R632^{LRP4}, the homologous residues for R953^{SORL1}, respectively. The structure of LRP5 has not been determined, but as the crystal structure of the highly homologous LRP6 has been solved[2, 11, 12], it allowed us to use these YWTD-domain structures to gain insight in the functional role of the arginine side chain for the arginines at blade-sequence position 38 as well as for the LRP5 residues (R494^{LRP5}/R481^{LRP6}; R752^{LRP5}/R739^{LRP6}; R1188^{LRP5}/R1178^{LRP6}) (**Figure 4e**). Indeed, we found that the arginine side chains in each of the domains are binding backbone carbonyls in the n-1 linker, and for 4 of the 5 structures a salt bridge to a glutamic acid (at domain position 28) assist in keeping the arginine properly positioned to make the main chain interactions to the n-1 linker residue (**Figure 4e**). This supports a disease mechanism where substitution of the arginine may lead to domain misfolding and destabilization in general, and importantly also for R953 of SORL1.

R953C disrupts SORL1 maturation and ectodomain shedding from the cell surface

SORL1 protein is synthesized in the ER and goes through a complex cellular process of maturation during trafficking in the ER and out of the Golgi into the ELN compartments and to the cell surface. The mature SORL1 isoform has complex-type *N*-glycosylations, and we previously showed only mature *N*-glycosylated SORL1 is shed from the cell surface to produce a fragment called soluble SORL1 (sSORL1)[14], and therefore a decrease in sSORL1 is often a direct measure of the maturation process being decreased for folding-deficient SORL1 mutant protein. Mature SORL1 migrates more slowly by SDS-PAGE, thus mature and immature isoforms of cellular SORL1 can be clearly distinguished[63] (**Figure 5a**).

To test whether the p.R953C variant affects SORL1 maturation and shedding, we transfected HEK293 and N2a cells with either the SORL1-WT or a SORL1-R953C construct. We performed Western blot analysis to determine the ratio of the mature to immature forms of the protein. We observed significantly decreased levels of mature SORL1 in HEK293 cells transfected with the R953C variant (**Figure 5a**). We next measured the level of sSORL1 in the culture medium of HEK293 and N2a cells, transiently transfected with expression constructs for SORL1-WT or SORL1-R953C. Compared to cells transfected with WT construct, we observed ~ 80% reduction in the sSORL1 level in the media from both the tested cell types transfected with the R953C construct (**Figure 5a, b**)

R953C reduces cell surface expression of SORL1

Because we observed a significant decrease in the shedding of SORL1-R953C, we tested whether the cell surface level of SORL1 could also be affected by this variant. We transiently transfected HEK293 cells with either SORL1-WT or SORL1-R953C and first analyzed cell surface levels of SORL1 using immunocytochemistry on unpermeabilized cells, which keeps the membrane intact to allow visualization of SORL1 protein solely located at the cell membrane. Using confocal microscopy, we observed considerably fewer cells expressing SORL1 at the cell surface in cells transfected with SORL1-R953C compared to SORL1-WT (**Figure 6a**). To quantitatively evaluate cell surface expression of SORL1-R953C relative to the total expression of the receptor in each individual cell, we used flow cytometry. We inserted the R953C variant into a C-terminally GFP tagged SORL1 construct, allowing for the detection of total expression of the receptor in each individual cell. We transfected both HEK293 cells and N2a cells and performed subsequent immunostaining of the transfected cells with anti-sSORL1 primary antibody and an Alexa Flour 647 secondary antibody in the absence of detergent to detect the cell surface expression of the receptor. These experiments demonstrated that more than 80% of the SORL1-R953C cells partially or completely retained SORL1 expression intracellularly compared to ~10-15% of the SORL1-WT cells. Results were consistent in both HEK293 and N2a cells (**Figure 6b-c**).

R953C prevents SORL1 from entering the endosomal recycling pathway

The differential cell surface localization and shedding of the R953C variant compared to WT led us to next investigate for possible changes in the intracellular localization of SORL1. For these experiments we transiently transfected HEK293 cells with either *SORL1*-WT or *SORL1*-R953C constructs. We analyzed co-localization of WT and R953C with two well-established endosomal markers, EEA1 (early endosome marker) and TFR (recycling endosome marker) and the ER marker Calnexin, 24 hours post-transfection. Using confocal microscopy, we demonstrated that the colocalization of R953C is strongly reduced with both endosomal markers (**Figure 7a-b**) and significantly increased in the ER (**Figure 7c**). Taken together, these data suggest that the R953C variant severely disrupts the normal cellular localization trafficking of SORL1 as would be expected if the mutation leads to defective protein folding.

Discussion

SORL1 is widely recognized as a strong AD risk gene though less is known about the AD risk attributable to rare missense variants[26, 55, 62]. Here we describe a family with two generations of both early and late onset AD in which we obtained brain autopsy pathology on 6 affected family members which enabled correlating clinical phenotype, genotype and neuropathology. Here we provide clinicopathological, genetic, and functional data supporting pathogenicity of a novel rare *SORL1* missense variant, p.(Arg953Cys) (R953C). Five of the five offspring were found to have the *SORL1* variant, and their age of onset ranged from 51yrs – 74 years. Notably, all affected individuals, including the mother who was WT for *SORL1* R953C, were of APOE3/3 genotype suggesting that APOE status was not contributing to risk or age of onset. Tissue from the mother (I-2) was analyzed by Sanger sequencing and found not to harbor R953C and tissue from the father was not available to confirm whether the allele was paternally inherited. Given the range of onset it is possible that additional genetic factors inherited from either parent has influenced expression of AD in both generations. Of note one living member of the family has been genotyped and is found to carry the variant (III-6) but is younger than the range of age of onset for the family. It is unknown whether her 3-year course of spasticity is related to the *SORL1* variant or is an unrelated case of a neurologic disease.

Neuropathology examination shows the presence of severe AD pathology, including extensive plaque and neurofibrillary tangle distribution. These histologic features typically correlate with advanced clinical disease[30, 52]. There are very few studies of neuropathology on *SORL1* variant carriers. There is one report of a *SORL1* homozygous truncating variant (c.364C>T, p.R122*) that shows severe cerebral amyloid angiopathy in addition to AD neuropathology as well as a patient with a splicing variant (c.4519+5G>A) in which AD was confirmed by neuropathological studies[5]. Yet another study shows SORL1 immunoreactivity in glial cells and white matter in a family with a *SORL1* variant c.3907C>T, p. R1303C.[69].

In our study, all cases underwent an extensive neuropathology examination in accordance with the most up-to-date guidelines for AD and related dementias[52, 53]. In this way, we were able to identify the presence of LATE-NC, marked by accumulation of TDP-43[53]. Interestingly, *SORL1* R953C segregated with LATE-NC pathology in 5 out of 5 offspring and with earlier age at AD

onset in 3 out of 5 offspring. In fact, a recent analysis linked carrying a variant in *SORL1* with LATE-NC[38]. Although LATE-NC is a common co-pathology identified in AD, the underlying etiology of this TDP-43 pathology is not well understood. Age seems to be the strongest risk factor and it is most frequently noticed in individuals older than 80 years[53, 54]. Similar to other age-related neuropathologic changes, LATE-NC frequently co-occurs with other pathologies such as AD and/or hippocampal sclerosis[6], and its presence may accelerate the cognitive decline associated with these disorders[37]. It is worth acknowledging that it is possible that the co-morbid pathology of LATE-NC is driving the earlier age of onset in this family. Additionally, Lewy body disease (LBD) was frequently observed in *SORL1* R953C carriers (**Figure 3**). One other report in the literature has associated SNPs in *SORL1* with LBD, but also implicates SNPs in *APOE* and *BIN1* in this association as well[17]. While LBD limited to the amygdala is frequently observed in association with advanced ADNC[30, 52], ADAD due to *PSEN1*, *PSEN2* and *APP* have been associated with brainstem, limbic and diffuse LBD[45, 48] similar to what we find in this family. However, it is possible SORL1 itself contributes directly to synuclein pathology. Together, these co-pathologies suggest that SORL1 R953C may be mechanistically linked to multiple proteinopathies, clinically manifesting as AD but also impacting TDP-43[38] and α-synuclein histopathology[17]. While SORL1 and a-synuclein have not been shown to directly interact, a-synuclein is internalized via clathrin-mediated endocytosis and is present in many arms of the endo-lysosomal network[67]. Loss of TDP-43 function affects recycling endosomes and impairs trophic signaling in neurons[64]. Therefore, while there might not be a direct interaction, dysfunction of SORL1 as an endosomal receptor that facilitates endosome sorting pathways may lead to more global impairments in endo-lysosomal network function that affect other proteins involved in neurodegeneration.

We performed analyses to examine cellular and extracellular levels of SORL1 as well as experiments to determine the localization of the R953C variant withing cells. Decreased SORL1 levels are known to be pathogenic as truncation variants leading to haploinsufficiency have been definitively linked to AD [25, 26, 62]. Furthermore, human neuronal models of *SORL1* deficiency show impairments in endosomal trafficking and recycling[28, 40, 51] as do neurons from minipigs with only one functional SORL1 allele[7]. One main function of SORL1 is to sort cargo from the early endosome to either the recycling pathway (cell surface) or the retrograde pathway (TGN) in

conjunction with the multi-protein complex retromer[22, 66]. The cellular localization of SORL1 and the cargo it binds depend on the specific isoform: monomer vs. dimer, mature vs. immature. For protein maturation, SORL1 transits through the Golgi and the trans-Golgi network to the endosome and to the cell surface. Here, we demonstrate that the R953C variant of SORL1 does not undergo maturation and is not shed from the cell surface.

We have recently found that two pathogenic *SORL1* missense variants associated with ADAD are located in either one of the CR-domains (Bjarnadottir et al., Manuscript in preparation) or the 3Fn-domains[35] respectively, and both display significantly impaired maturation and shedding. We have also previously observed that sSORL1 is significantly decreased in the CSF from several carriers of other established pathogenic SORL1 variants (Andersen lab, unpublished data). Furthermore, a larger screen of 70 SORL1 coding variants suggested that impaired maturation may be a common dysfunction of SORL1 mutant proteins[60].

Our study suggests that SORL1 R953C likely cannot function as a normal endosomal receptor, as it fails to enter the endosomal pathway. Instead, it is sequestered in the ER. When the receptor gets retained in the ER, it will lead to a decrease in SORL1 activity in endosomal compartments, so a direct effect of ER retention is lack-of-activity of SORL1 in the endo-lysosomal pathway. However, there could also be a gain-of-toxic-activity associated with the ER retained misfolded receptor that potentially could lead to neurotoxic ER-stress, which is suggested to occur with certain pathogenic variants in the homologous LDLR[39, 68]. Furthermore, the ER-retained SORL1 mutant protein may have additional negative impacts on total receptor activity in the endosome and thus increase the pathogenicity of the variant. In this scenario, the mutated receptor could dimerize (or even polymerize) with the wild-type receptor, thus sequestering additional wild-type SORL1 in the ER, potentially acting via a dominant-negative mechanism in diploid cells. Structural analysis indicates that this variant occurs at a critical arginine in the YWTD β-propeller domain of SORL1 that appears to be necessary for the proper folding of the domain. When compared against homologous domains in the LDLR receptor family, arginine substitutions at this position are strongly suspected to be pathogenic.

Finally, we demonstrate that this variant likely impedes SORL1 from entering the endosomal sorting pathway. SORL1 is an endosomal receptor for many proteins that are important for proper

neuronal function. We and others have shown that loss of SORL1 leads to endosomal 'traffic jams' and mis-localization of neurotrophic receptors and glutamate receptor subunits[51]. Loss of SORL1 in the endosomal sorting pathway will likely affect multiple aspects of neuronal health and function, contributing to neurodegeneration.

Over 500 variants in *SORL1* have been identified and recent genetic studies have provided evidence as to which variants may be likely pathogenic or likely benign[25]. However, with such a large gene (encoding for more than 2200 amino acids), more variants are likely to be identified. Functional analysis of *SORL1* variants will be an important tool to classify these variants based on their cellular pathogenicity and further uncover their contribution to the development of AD.

Acknowledgements

The authors are grateful to the family whose participation made this work possible.

Flow cytometry was performed at the FACS Core Facility, Aarhus University, Denmark.
The authors acknowledge AU Health Bioimaging Core Facility for the use of equipment and support of the imaging facility.

The authors thank the members of the University of Washington Medicine Center for Precision Diagnostics for technical support, the Geriatric Research, Education, and Clinical Center at the VA Puget Sound Health Care System, and University of Washington's Alzheimer Disease Research Center.

We acknowledge Harald Frankowski in the Young lab for preparation of gDNA samples for SORL1 variant sequencing and all members of the Young lab for helpful discussions on this work.

Funding

O.M.A is supported by Novo Nordisk Foundation (#NNF20OC0064162), the Alzheimer's Association (ADSF-21-831378-C), the EU Joint Programme-Neurodegenerative Disease Research (JPND) Working Group SORLA-FIX under the 2019 ''Personalized Medicine'' call (funded in part by the Danish Innovation Foundation and the Velux Foundation Denmark), and the Danish Alzheimer's Research Foundation (recipient of the 2022 Basic Research Science Award).

J.E.Y is supported by NIH grants R01 AG062148, K01 AG059841; an Alzheimer's Association Research Grant 23AARG1022491; a Sponsored Research Agreement from Retromer Therapeutics and a generous gift from the Ellison Foundation (to UW).
D.D.C. is supported by the Alzheimer's Disease Training Program (ADTP): T32 AG052354-06A1
Clinical and pathological work is supported by the Alzheimer's Disease Research Center (P30 AG05136)

Competing Interests

O.M.A. is a consultant for Retromer Therapeutics and has equity. The other authors report no competing interests.

References

1 Abdel-Hamid MS, Elhossini RM, Otaify GA, Abdel-Ghafar SF, Aglan MS (2022) Osteoporosis-pseudoglioma syndrome in four new patients: identification of two novel LRP5 variants and insights on patients' management using bisphosphonates therapy. Osteoporos Int 33: 1501-1510 Doi 10.1007/s00198-022-06313-1

2 Ahn VE, Chu ML, Choi HJ, Tran D, Abo A, Weis WI (2011) Structural basis of Wnt signaling inhibition by Dickkopf binding to LRP5/6. Dev Cell 21: 862-873 Doi 10.1016/j.devcel.2011.09.003

3 Ai M, Heeger S, Bartels CF, Schelling DK, Osteoporosis-Pseudoglioma Collaborative G (2005) Clinical and molecular findings in osteoporosis-pseudoglioma syndrome. Am J Hum Genet 77: 741-753 Doi 10.1086/497706

4 Alonso N, Soares DC, E VM, Summers GD, Ralston SH, Gregson CL (2015) Atypical femoral fracture in osteoporosis pseudoglioma syndrome associated with two novel compound heterozygous mutations in LRP5. J Bone Miner Res 30: 615-620 Doi 10.1002/jbmr.2403

5 Alvarez-Mora MI, Blanco-Palmero VA, Quesada-Espinosa JF, Arteche-Lopez AR, Llamas-Velasco S, Palma Milla C, Lezana Rosales JM, Gomez-Manjon I, Hernandez-Lain A, Jimenez Almonacid Jet al (2022) Heterozygous and Homozygous Variants in SORL1 Gene in Alzheimer's Disease Patients: Clinical, Neuroimaging and Neuropathological Findings. Int J Mol Sci 23: Doi 10.3390/ijms23084230

6 Amador-Ortiz C, Lin WL, Ahmed Z, Personett D, Davies P, Duara R, Graff-Radford NR, Hutton ML, Dickson DW (2007) TDP-43 immunoreactivity in hippocampal sclerosis and Alzheimer's disease. Ann Neurol 61: 435-445 Doi 10.1002/ana.21154

7 Andersen OM, Bogh N, Landau AM, Ploen GG, Jensen AMG, Monti G, Ulhoi BP, Nyengaard JR, Jacobsen KR, Jorgensen MMet al (2022) A genetically modified minipig model for Alzheimer's disease with SORL1 haploinsufficiency. Cell Rep Med 3: 100740 Doi 10.1016/j.xcrm.2022.100740

8 Andersen OM, Monti, G, Jensen A.M.G., de Waal, M., Hulsman, M., Olsen J.G., Holstege, H. (2023) Relying on the relationship with known disease-causing variants in homologus proteins to predict pathogenicity of SORL1 variants in Alzheimer's disease. BioRxiv doi.org/10.1101/2023.02.27.524103:

9 Baker E, Leonenko G, Schmidt KM, Hill M, Myers AJ, Shoai M, de Rojas I, Tesi N, Holstege H, van der Flier WMet al (2023) What does heritability of Alzheimer's disease represent? PLoS One 18: e0281440 Doi 10.1371/journal.pone.0281440

10 Bell MD, Long T, Roden AC, Cooper FI, Sanchez H, Trower C, Martinez C, Hooper JE, Autopsy Committee of the College of American P (2022) Updating Normal Organ Weights

Using a Large Current Sample Database. Arch Pathol Lab Med 146: 1486-1495 Doi 10.5858/arpa.2021-0287-OA

11 Bourhis E, Wang W, Tam C, Hwang J, Zhang Y, Spittler D, Huang OW, Gong Y, Estevez A, Zilberleyb Iet al (2011) Wnt antagonists bind through a short peptide to the first beta-propeller domain of LRP5/6. Structure 19: 1433-1442 Doi 10.1016/j.str.2011.07.005

12 Cheng Z, Biechele T, Wei Z, Morrone S, Moon RT, Wang L, Xu W (2011) Crystal structures of the extracellular domain of LRP6 and its complex with DKK1. Nat Struct Mol Biol 18: 1204-1210 Doi 10.1038/nsmb.2139

13 Chiou KR, Charng MJ (2010) Detection of mutations and large rearrangements of the low-density lipoprotein receptor gene in Taiwanese patients with familial hypercholesterolemia. Am J Cardiol 105: 1752-1758 Doi 10.1016/j.amjcard.2010.01.356

14 Christensen S, Narimatsu, Y., Simoes S., Goth CK., Vaegter CB., Small SA., Clausen H., Andersen, OM. (2020) Endosomal trafficking is required for glycosylation and normal maturation of the Alzheimer's-associated protein sorLA. BioRxiv: Doi https://doi.org/10.1101/2020.07.12.199885

15 Cingolani P, Platts A, Wang le L, Coon M, Nguyen T, Wang L, Land SJ, Lu X, Ruden DM (2012) A program for annotating and predicting the effects of single nucleotide polymorphisms, SnpEff: SNPs in the genome of Drosophila melanogaster strain w1118; iso-2; iso-3. Fly (Austin) 6: 80-92 Doi 10.4161/fly.19695

16 Cnossen WR, te Morsche RH, Hoischen A, Gilissen C, Chrispijn M, Venselaar H, Mehdi S, Bergmann C, Veltman JA, Drenth JP (2014) Whole-exome sequencing reveals LRP5 mutations and canonical Wnt signaling associated with hepatic cystogenesis. Proc Natl Acad Sci U S A 111: 5343-5348 Doi 10.1073/pnas.1309438111

17 Dai DL, Tropea TF, Robinson JL, Suh E, Hurtig H, Weintraub D, Van Deerlin V, Lee EB, Trojanowski JQ, Chen-Plotkin AS (2020) ADNC-RS, a clinical-genetic risk score, predicts Alzheimer's pathology in autopsy-confirmed Parkinson's disease and Dementia with Lewy bodies. Acta Neuropathol 140: 449-461 Doi 10.1007/s00401-020-02199-7

18 Daly JL, Danson CM, Lewis PA, Zhao L, Riccardo S, Di Filippo L, Cacchiarelli D, Lee D, Cross SJ, Heesom KJet al (2023) Multi-omic approach characterises the neuroprotective role of retromer in regulating lysosomal health. Nat Commun 14: 3086 Doi 10.1038/s41467-023-38719-8

19 DePristo MA, Banks E, Poplin R, Garimella KV, Maguire JR, Hartl C, Philippakis AA, del Angel G, Rivas MA, Hanna Met al (2011) A framework for variation discovery and genotyping using next-generation DNA sequencing data. Nat Genet 43: 491-498 Doi 10.1038/ng.806

20 Descamps OS, Gilbeau JP, Leysen X, Van Leuven F, Heller FR (2001) Impact of genetic defects on atherosclerosis in patients suspected of familial hypercholesterolaemia. Eur J Clin Invest 31: 958-965 Doi 10.1046/j.1365-2362.2001.00915.x

21 Dumanis SB, Burgert T, Caglayan S, Fuchtbauer A, Fuchtbauer EM, Schmidt V, Willnow TE (2015) Distinct Functions for Anterograde and Retrograde Sorting of SORLA in Amyloidogenic Processes in the Brain. J Neurosci 35: 12703-12713 Doi 10.1523/JNEUROSCI.0427-15.2015

22 Fjorback AW, Seaman M, Gustafsen C, Mehmedbasic A, Gokool S, Wu C, Militz D, Schmidt V, Madsen P, Nyengaard JRet al (2012) Retromer binds the FANSHY sorting motif in SorLA

to regulate amyloid precursor protein sorting and processing. J Neurosci 32: 1467-1480 Doi 10.1523/JNEUROSCI.2272-11.2012

23 Gong Y, Slee RB, Fukai N, Rawadi G, Roman-Roman S, Reginato AM, Wang H, Cundy T, Glorieux FH, Lev Det al (2001) LDL receptor-related protein 5 (LRP5) affects bone accrual and eye development. Cell 107: 513-523 Doi 10.1016/s0092-8674(01)00571-2

24 Herskowitz JH, Offe K, Deshpande A, Kahn RA, Levey AI, Lah JJ (2012) GGA1-mediated endocytic traffic of LR11/SorLA alters APP intracellular distribution and amyloid-beta production. Mol Biol Cell 23: 2645-2657 Doi 10.1091/mbc.E12-01-0014

25 Holstege H, Hulsman M, Charbonnier C, Grenier-Boley B, Quenez O, Grozeva D, van Rooij JGJ, Sims R, Ahmad S, Amin Net al (2022) Exome sequencing identifies rare damaging variants in ATP8B4 and ABCA1 as risk factors for Alzheimer's disease. Nat Genet 54: 1786-1794 Doi 10.1038/s41588-022-01208-7

26 Holstege H, van der Lee SJ, Hulsman M, Wong TH, van Rooij JG, Weiss M, Louwersheimer E, Wolters FJ, Amin N, Uitterlinden AGet al (2017) Characterization of pathogenic SORL1 genetic variants for association with Alzheimer's disease: a clinical interpretation strategy. Eur J Hum Genet 25: 973-981 Doi 10.1038/ejhg.2017.87

27 Hull S, Arno G, Ostergaard P, Pontikos N, Robson AG, Webster AR, Hogg CR, Wright GA, Henderson RHH, Martin CAet al (2019) Clinical and Molecular Characterization of Familial Exudative Vitreoretinopathy Associated With Microcephaly. Am J Ophthalmol 207: 87-98 Doi 10.1016/j.ajo.2019.05.001

28 Hung C, Tuck E, Stubbs V, van der Lee SJ, Aalfs C, van Spaendonk R, Scheltens P, Hardy J, Holstege H, Livesey FJ (2021) SORL1 deficiency in human excitatory neurons causes APP-dependent defects in the endolysosome-autophagy network. Cell Rep 35: 109259 Doi 10.1016/j.celrep.2021.109259

29 Huybrechts Y, Boudin E, Hendrickx G, Steenackers E, Hamdy N, Mortier G, Martinez Diaz-Guerra G, Bracamonte MS, Appelman-Dijkstra NM, Van Hul W (2021) Identification of Compound Heterozygous Variants in LRP4 Demonstrates That a Pathogenic Variant outside the Third beta-Propeller Domain Can Cause Sclerosteosis. Genes (Basel) 13: Doi 10.3390/genes13010080

30 Hyman BT, Phelps CH, Beach TG, Bigio EH, Cairns NJ, Carrillo MC, Dickson DW, Duyckaerts C, Frosch MP, Masliah Eet al (2012) National Institute on Aging-Alzheimer's Association guidelines for the neuropathologic assessment of Alzheimer's disease. Alzheimers Dement 8: 1-13 Doi 10.1016/j.jalz.2011.10.007

31 Jacobsen L, Madsen P, Jacobsen C, Nielsen MS, Gliemann J, Petersen CM (2001) Activation and functional characterization of the mosaic receptor SorLA/LR11. J Biol Chem 276: 22788-22796 Doi 10.1074/jbc.M100857200

32 Jacobsen L, Madsen P, Moestrup SK, Lund AH, Tommerup N, Nykjaer A, Sottrup-Jensen L, Gliemann J, Petersen CM (1996) Molecular characterization of a novel human hybrid-type receptor that binds the alpha2-macroglobulin receptor-associated protein. J Biol Chem 271: 31379-31383 Doi 10.1074/jbc.271.49.31379

33 Jayadev S (2022) Genetics of Alzheimer Disease. Continuum (Minneap Minn) 28: 852-871 Doi 10.1212/CON.0000000000001125

34 Jensen AMG, Kitago Y, Fazeli E, Vaegter CB, Small SA, Petsko GA, Andersen OM (2023) Dimerization of the Alzheimer's disease pathogenic receptor SORLA regulates its

association with retromer. Proc Natl Acad Sci U S A 120: e2212180120 Doi 10.1073/pnas.2212180120

35 Jensen AMG, Raska J., Fojtik P., Monti G., Lunding M., Vochyanova S., Pospisilova V., van der Lee S.J., Van Dongen J., Bossaerts L., Van Broeckhoven C., Dols O., Lleo A., Benussi, L., Ghidoni R., Hulsman M., Sleegers K., Bohaciakova D., Holstege H., Andersen O.M. (2023) The SORL1 p. Y1816C variant causes impaired endosomal dimerization and autosomal dominant Alzheimer's disease. MedRxiv: Doi 10.1101/2023.07.09.23292253

36 Jiao X, Ventruto V, Trese MT, Shastry BS, Hejtmancik JF (2004) Autosomal recessive familial exudative vitreoretinopathy is associated with mutations in LRP5. Am J Hum Genet 75: 878-884 Doi 10.1086/425080

37 Josephs KA, Whitwell JL, Tosakulwong N, Weigand SD, Murray ME, Liesinger AM, Petrucelli L, Senjem ML, Ivnik RJ, Parisi JEet al (2015) TAR DNA-binding protein 43 and pathological subtype of Alzheimer's disease impact clinical features. Ann Neurol 78: 697-709 Doi 10.1002/ana.24493

38 Katsumata Y, Shade LM, Hohman TJ, Schneider JA, Bennett DA, Farfel JM, Alzheimer's Disease Genetics C, Kukull WA, Fardo DW, Nelson PT (2022) Multiple gene variants linked to Alzheimer's-type clinical dementia via GWAS are also associated with non-Alzheimer's neuropathologic entities. Neurobiol Dis 174: 105880 Doi 10.1016/j.nbd.2022.105880

39 Kizhakkedath P, John A, Al-Sawafi BK, Al-Gazali L, Ali BR (2019) Endoplasmic reticulum quality control of LDLR variants associated with familial hypercholesterolemia. FEBS Open Bio 9: 1994-2005 Doi 10.1002/2211-5463.12740

40 Knupp A, Mishra S, Martinez R, Braggin JE, Szabo M, Kinoshita C, Hailey DW, Small SA, Jayadev S, Young JE (2020) Depletion of the AD Risk Gene SORL1 Selectively Impairs Neuronal Endosomal Traffic Independent of Amyloidogenic APP Processing. Cell Rep 31: 107719 Doi 10.1016/j.celrep.2020.107719

41 Kopanos C, Tsiolkas V, Kouris A, Chapple CE, Albarca Aguilera M, Meyer R, Massouras A (2019) VarSome: the human genomic variant search engine. Bioinformatics 35: 1978-1980 Doi 10.1093/bioinformatics/bty897

42 Kunkle BW, Grenier-Boley B, Sims R, Bis JC, Damotte V, Naj AC, Boland A, Vronskaya M, van der Lee SJ, Amlie-Wolf Aet al (2019) Genetic meta-analysis of diagnosed Alzheimer's disease identifies new risk loci and implicates Abeta, tau, immunity and lipid processing. Nat Genet 51: 414-430 Doi 10.1038/s41588-019-0358-2

43 Lambert JC, Ibrahim-Verbaas CA, Harold D, Naj AC, Sims R, Bellenguez C, Jun G, Destefano AL, Bis JC, Beecham GWet al (2013) Meta-analysis of 74,046 individuals identifies 11 new susceptibility loci for Alzheimer's disease. Nat Genet 45: 1452-1458 Doi 10.1038/ng.2802

44 Lee EG, Tulloch J, Chen S, Leong L, Saxton AD, Kraemer B, Darvas M, Keene CD, Shutes-David A, Todd Ket al (2020) Redefining transcriptional regulation of the APOE gene and its association with Alzheimer's disease. PLoS One 15: e0227667 Doi 10.1371/journal.pone.0227667

45 Leverenz JB, Fishel MA, Peskind ER, Montine TJ, Nochlin D, Steinbart E, Raskind MA, Schellenberg GD, Bird TD, Tsuang D (2006) Lewy body pathology in familial Alzheimer disease: evidence for disease- and mutation-specific pathologic phenotype. Arch Neurol 63: 370-376 Doi 10.1001/archneur.63.3.370

46 Li H, Durbin R (2009) Fast and accurate short read alignment with Burrows-Wheeler transform. Bioinformatics 25: 1754-1760 Doi 10.1093/bioinformatics/btp324

47 Li JK, Li Y, Zhang X, Chen CL, Rao YQ, Fei P, Zhang Q, Zhao P, Li J (2018) Spectrum of Variants in 389 Chinese Probands With Familial Exudative Vitreoretinopathy. Invest Ophthalmol Vis Sci 59: 5368-5381 Doi 10.1167/iovs.17-23541

48 Lippa CF, Fujiwara H, Mann DM, Giasson B, Baba M, Schmidt ML, Nee LE, O'Connell B, Pollen DA, St George-Hyslop Pet al (1998) Lewy bodies contain altered alpha-synuclein in brains of many familial Alzheimer's disease patients with mutations in presenilin and amyloid precursor protein genes. Am J Pathol 153: 1365-1370 Doi 10.1016/s0002-9440(10)65722-7

49 McKenna A, Hanna M, Banks E, Sivachenko A, Cibulskis K, Kernytsky A, Garimella K, Altshuler D, Gabriel S, Daly M, DePristo MA (2010) The Genome Analysis Toolkit: a MapReduce framework for analyzing next-generation DNA sequencing data. Genome Res 20: 1297-1303 Doi 10.1101/gr.107524.110

50 Miguel L, Gervais J, Nicolas G, Lecourtois M (2023) SorLA Protective Function Is Restored by Improving SorLA Protein Maturation in a Subset of Alzheimer's Disease-Associated SORL1 Missense Variants. J Alzheimers Dis 94: 1343-1349 Doi 10.3233/JAD-230211

51 Mishra S, Knupp A, Szabo MP, Williams CA, Kinoshita C, Hailey DW, Wang Y, Andersen OM, Young JE (2022) The Alzheimer's gene SORL1 is a regulator of endosomal traffic and recycling in human neurons. Cell Mol Life Sci 79: 162 Doi 10.1007/s00018-022-04182-9

52 Montine TJ, Phelps CH, Beach TG, Bigio EH, Cairns NJ, Dickson DW, Duyckaerts C, Frosch MP, Masliah E, Mirra SSet al (2012) National Institute on Aging-Alzheimer's Association guidelines for the neuropathologic assessment of Alzheimer's disease: a practical approach. Acta Neuropathol 123: 1-11 Doi 10.1007/s00401-011-0910-3

53 Nelson PT, Dickson DW, Trojanowski JQ, Jack CR, Boyle PA, Arfanakis K, Rademakers R, Alafuzoff I, Attems J, Brayne Cet al (2019) Limbic-predominant age-related TDP-43 encephalopathy (LATE): consensus working group report. Brain 142: 1503-1527 Doi 10.1093/brain/awz099

54 Nelson PT, Lee EB, Cykowski MD, Alafuzoff I, Arfanakis K, Attems J, Brayne C, Corrada MM, Dugger BN, Flanagan MEet al (2023) LATE-NC staging in routine neuropathologic diagnosis: an update. Acta Neuropathol 145: 159-173 Doi 10.1007/s00401-022-02524-2

55 Pottier C, Hannequin D, Coutant S, Rovelet-Lecrux A, Wallon D, Rousseau S, Legallic S, Paquet C, Bombois S, Pariente Jet al (2012) High frequency of potentially pathogenic SORL1 mutations in autosomal dominant early-onset Alzheimer disease. Mol Psychiatry 17: 875-879 Doi 10.1038/mp.2012.15

56 Raghavan NS, Brickman AM, Andrews H, Manly JJ, Schupf N, Lantigua R, Wolock CJ, Kamalakaran S, Petrovski S, Tosto Get al (2018) Whole-exome sequencing in 20,197 persons for rare variants in Alzheimer's disease. Ann Clin Transl Neurol 5: 832-842 Doi 10.1002/acn3.582

57 Reitz C (2018) Retromer Dysfunction and Neurodegenerative Disease. Curr Genomics 19: 279-288 Doi 10.2174/1389202919666171024122809

58 Reitz C, Cheng R, Rogaeva E, Lee JH, Tokuhiro S, Zou F, Bettens K, Sleegers K, Tan EK, Kimura Ret al (2011) Meta-analysis of the association between variants in SORL1 and Alzheimer disease. Arch Neurol 68: 99-106 Doi 10.1001/archneurol.2010.346

59 Rogaeva E, Meng Y, Lee JH, Gu Y, Kawarai T, Zou F, Katayama T, Baldwin CT, Cheng R, Hasegawa Het al (2007) The neuronal sortilin-related receptor SORL1 is genetically associated with Alzheimer disease. Nat Genet 39: 168-177 Doi 10.1038/ng1943

60 Rovelet-Lecrux A, Feuillette S, Miguel L, Schramm C, Pernet S, Quenez O, Segalas-Milazzo I, Guilhaudis L, Rousseau S, Riou Get al (2021) Impaired SorLA maturation and trafficking as a new mechanism for SORL1 missense variants in Alzheimer disease. Acta Neuropathol Commun 9: 196 Doi 10.1186/s40478-021-01294-4

61 Rudenko G, Henry L, Henderson K, Ichtchenko K, Brown MS, Goldstein JL, Deisenhofer J (2002) Structure of the LDL receptor extracellular domain at endosomal pH. Science 298: 2353-2358 Doi 10.1126/science.1078124

62 Scheltens P, De Strooper B, Kivipelto M, Holstege H, Chetelat G, Teunissen CE, Cummings J, van der Flier WM (2021) Alzheimer's disease. Lancet 397: 1577-1590 Doi 10.1016/S0140-6736(20)32205-4

63 Schmidt V, Sporbert A, Rohe M, Reimer T, Rehm A, Andersen OM, Willnow TE (2007) SorLA/LR11 regulates processing of amyloid precursor protein via interaction with adaptors GGA and PACS-1. J Biol Chem 282: 32956-32964 Doi 10.1074/jbc.M705073200

64 Schwenk BM, Hartmann H, Serdaroglu A, Schludi MH, Hornburg D, Meissner F, Orozco D, Colombo A, Tahirovic S, Michaelsen Met al (2016) TDP-43 loss of function inhibits endosomal trafficking and alters trophic signaling in neurons. EMBO J 35: 2350-2370 Doi 10.15252/embj.201694221

65 Simoes S, Guo J, Buitrago L, Qureshi YH, Feng X, Kothiya M, Cortes E, Patel V, Kannan S, Kim YHet al (2021) Alzheimer's vulnerable brain region relies on a distinct retromer core dedicated to endosomal recycling. Cell Rep 37: 110182 Doi 10.1016/j.celrep.2021.110182

66 Small SA, Kent K, Pierce A, Leung C, Kang MS, Okada H, Honig L, Vonsattel JP, Kim TW (2005) Model-guided microarray implicates the retromer complex in Alzheimer's disease. Ann Neurol 58: 909-919 Doi 10.1002/ana.20667

67 Smith JK, Mellick GD, Sykes AM (2022) The role of the endolysosomal pathway in alpha-synuclein pathogenesis in Parkinson's disease. Front Cell Neurosci 16: 1081426 Doi 10.3389/fncel.2022.1081426

68 Sorensen S, Ranheim T, Bakken KS, Leren TP, Kulseth MA (2006) Retention of mutant low density lipoprotein receptor in endoplasmic reticulum (ER) leads to ER stress. J Biol Chem 281: 468-476 Doi 10.1074/jbc.M507071200

69 Thonberg H, Chiang HH, Lilius L, Forsell C, Lindstrom AK, Johansson C, Bjorkstrom J, Thordardottir S, Sleegers K, Van Broeckhoven Cet al (2017) Identification and description of three families with familial Alzheimer disease that segregate variants in the SORL1 gene. Acta Neuropathol Commun 5: 43 Doi 10.1186/s40478-017-0441-9

70 Tosto G, Reitz C (2013) Genome-wide association studies in Alzheimer's disease: a review. Curr Neurol Neurosci Rep 13: 381 Doi 10.1007/s11910-013-0381-0

71 Verheijen J, Van den Bossche T, van der Zee J, Engelborghs S, Sanchez-Valle R, Llado A, Graff C, Thonberg H, Pastor P, Ortega-Cubero Set al (2016) A comprehensive study of the genetic impact of rare variants in SORL1 in European early-onset Alzheimer's disease. Acta Neuropathol 132: 213-224 Doi 10.1007/s00401-016-1566-9

72 Willnow TE, Petersen CM, Nykjaer A (2008) VPS10P-domain receptors - regulators of neuronal viability and function. Nat Rev Neurosci 9: 899-909 Doi nrn2516 [pii]

10.1038/nrn2516

73 Yamazaki H, Bujo H, Kusunoki J, Seimiya K, Kanaki T, Morisaki N, Schneider WJ, Saito Y (1996) Elements of neural adhesion molecules and a yeast vacuolar protein sorting receptor are present in a novel mammalian low density lipoprotein receptor family member. J Biol Chem 271: 24761-24768 Doi 10.1074/jbc.271.40.24761

74 Yamazaki H, Bujo H, Saito Y (1997) A novel member of the LDL receptor gene family with eleven binding repeats is structurally related to neural adhesion molecules and a yeast vacuolar protein sorting receptor. J Atheroscler Thromb 4: 20-26

75 Zong Y, Zhang B, Gu S, Lee K, Zhou J, Yao G, Figueiredo D, Perry K, Mei L, Jin R (2012) Structural basis of agrin-LRP4-MuSK signaling. Genes Dev 26: 247-258 Doi 10.1101/gad.180885.111

Figure Legends

Figure 1. Pedigree of SORL1 R953C family: Solid black indicates individuals diagnosed with Alzheimer Disease which was confirmed by neuropathology. Dark grey indicates clinical diagnosis of dementia. Onset of disease ("o" years) and age at death "d" years is indicated next to the individual when applicable. Circles indicate female, square indicates male. Diamond is sex unknown to investigators at time of report. + or – indicates presence or absence of *SORL1* c.2857C>T variant. In individuals where APOE genotype was assessed it is indicated on pedigree.

Figure 2. Neuropathologic evaluation demonstrates high Alzheimer disease pathologic change (ADNC) by NIA-AA criteria in SORL1 R953C cases. (a) Representative section of cerebellum stained for β-amyloid (6e10), highlighting plaques within the molecular layer and warranting a Thal phase 5. Patient II-5, scale bar = 50 μm. (b) Representative section of calcarine cortex stained for phosphorylated tau (P-Tau; AT8), highlighting neurofibrillary tangles in a background of dystrophic neurites, consistent with Braak and Braak stage VI. Patient II-5, scale bar = 20 μm. (c) Representative section of middle frontal gyrus stained with Bielschowsky silver

demonstrating frequent neuritic plaques by CERAD criteria. Insert shows a representative neuritic plaque, composed of brown, targetoid β-amyloid associated with black dystrophic neurites. Patient II-5, scale bars = 50 μm. (d) Representative section of hippocampus stained for phosphorylated TDP-43 (P-TDP43), demonstrating intracytoplasmic inclusions and scattered dystrophic neurites. The pattern is consistent with limbic-predominant age-related TDP-43 encephalopathy (LATE) stage 2, though age < 80 years is atypical for sporadic LATE. Patient II-4, scale bar = 20 μm. (e) Representative section of anterior cingulate gyrus stained for α-synuclein, highlighting the presence of a Lewy body in a background of positive neurites. Though Lewy body disease was present in the majority of SORL1 R953C carriers, the pattern was highly variable. Patient II-2, scale bar = 20 μm.

Figure 3. Neuropathology of all family members who consented to autopsy.
Representative photomicrographs demonstrating highest level neuropathologic change in each autopsy case for β-amyloid plaques (6e10 antibody), neurofibrillary tangles (tau antibodies as listed below), neuritic plaques (Bielschowsky silver stain), phosphorylated-TDP-43 inclusions (P-TDP43 antibody), and Lewy bodies (α-Synuclein antibody). (a) Patient I-2, with β-amyloid plaques in the substantia nigra, neurofibrillary tangles (Tau2 antibody) in the calcarine cortex (primary visual cortex), and frequent neuritic plaque density by CERAD criteria (note that silver staining was lighter than other cases). No p-TDP43 or α-synuclein was present, shown here as lack of staining in areas affected early in disease process. (b) Patient II-1, with β-amyloid plaques in the periaqueductal grey matter of the midbrain, neurofibrillary tangles (AT8 antibody) in the calcarine cortex, and frequent neuritic plaque density by CERAD criteria. P-TDP43 inclusions were present in the hippocampus, highlighted by arrows. Lewy bodies were present in brainstem, amygdala, limbic structures, and frontal cortex (shown here). (c) Patient II-2, with β-amyloid plaques in the cerebellum, neurofibrillary tangles in the calcarine cortex (AT8 antibody), and frequent neuritic plaque density by CERAD criteria. P-TDP43 inclusions were present in the hippocampus. Lewy bodies were present in the amygdala and substantia nigra, consistent with a limbic (transitional) pattern. (d) Patient II-3, with β-amyloid plaques in the cerebellum, neurofibrillary tangles in the middle frontal gyrus (AT8 antibody), and frequent neuritic plaque density by CERAD criteria. P-TDP43 inclusions were present in amygdala neurites. No Lewy bodies were observed, demonstrated here by negative staining of the olfactory bulb, one of the

earliest anatomic sites of Lewy body formation. (e) Patient II-4, with β-amyloid plaques in the cerebellum, neurofibrillary tangles in the calcarine cortex (Tau2 antibody), and frequent neuritic plaque density by CERAD criteria. P-TDP43 inclusions were present in the hippocampus. Lewy bodies were present in the pigmented cells of the substantia nigra but not in any other site. (f) Patient II-5, with β-amyloid plaques in the cerebellum, neurofibrillary tangles in the calcarine cortex (Tau2 antibody), and frequent neuritic plaque density by CERAD criteria. P-TDP43 inclusions were present in the hippocampus. No Lewy bodies were observed, again demonstrated here by negative staining of the olfactory bulb. Scale bars = 20 μm for β-amyloid, p-tau, p-TDP43, and α-Synuclein; scale bars = 50 μm for Bielschowsky silver stain.

Figure 4. *In silico* characterization of SORL1 p. R953C

(a) Schematic presentation of the mosaic domain structure of the SORL1 protein comprising from the N-terminal end: VPS10p-domain with accompanying 10CCa/b domains, YWTD-repeated β-propeller domain (with p.R953C location indicated) with accompanying EGF-domain, cluster of 11 CR-domains, cluster of 6 3Fn-domains, a transmembrane domain followed by a cytoplasmic tail at the C-terminal end. (b) Three-dimensional model of the SORL1 YWTD-domain folding prepared from coordinates from ModelArchive (Y.Kitago, O.M. Andersen, G.A. Petsko. ModelArchive: https://modelarchiveorg/doi/10.5452/ma-agbg4). (c) Alignment of the ~40 amino acids from each of the six YWTD-repeated sequences corresponding to the blades of the β-propeller with indication of β-strands in grey. The arginine R953 resides at domain position 38 of the sequence located in the loop between strands C and D of the fifth β-blade. Partly conserved domain positions are indicated with bold letters and the consensus residues below the SORL1 alignment. Below 5 sequences of YWTD-repeated sequences from homologous receptor proteins with known pathogenic variants corresponding to arginines at position 38. (d) The side chain of Arg-953 from SORL1 provides structural stabilization of the domain folding by an ionic interaction with the side chain of Glu-943 based on the three-dimensional model of the folded YWTD-domain. (e) Close-up of the Arg-Glu pairs from YWTD-domain crystal structures for residues in LDLR, LRP4 and LRP6 (LRP5 homolog) corresponding to pathogenic variants as listed in panel c

Figure 5. SORL1 R953C cells are defective in maturation and shedding of the SORL1 protein.

(a) Representative western blotting of lysate and media samples from HEK293 cells transiently transfected with SORLA-WT or SORLA-R953C. (b) Densitometric analysis from HEK293 and N2a samples. The signal for the R953C is expressed relative to the WT signal. Results are expressed as Mean± SD and analyzed by parametric two-tailed paired t-test. Significance was defined as a value of **p<0. 01, ***p<0. 001. n= 4 independent experiments

Figure 6. SORL1 R953C cells have reduced SORL1 protein localization on the cell surface.

(a) Representative immunocytochemistry from HEK293 cells transiently transfected with SORLA-WT or SORLA-R953C expression construct and stained for SORLA (red) at the cell surface. White arrows show positive cells. (b) Flow cytometry dot plot showing surface (AlexaFluor 647 fluorescence) and total (GFP fluorescence) in live single HEK293 cells expressing WT-GFP and R953C-GFP. Vertical and horizontal lines represent thresholds for GFP and AlexaFluor 647-positive cells, respectively. Represented are GFP-positive cells with AlexaFluor 647 signal above (black, inside red dashed gate) or below threshold (dark grey); and untransfected cells (light grey). Numbers in the plots represent the percentages of the cells inside the gates. (c) Bar plots of AlexaFluor 647 fluorescence in HEK293 and N2a cells expressing WT-GFP or R953C-GFP, generated from population of GFP-positive cells. n=3 independent experiments. Results are expressed as Mean± SD and analyzed by parametric two-tailed paired t-test. Significance was defined as a value of ***p<0. 001.

Figure 7. SORL1 R953C cells have reduced localization of the SORL1 protein in early and recycling endosomes. HEK293 cells transiently expressing WT or R953C (red) are shown for their colocalization with (a) EEA1 (early endosomal marker), (b) TFR (recycling endosomal marker), and (c) Calnexin (ER marker) (green). The nuclei were visualized with Hoechst (blue). Bar graphs on the right panel illustrate quantifications of colocalization between WT and R953C in cells co-stained for (a) EEA1, (b) TFR and (c) Calnexin. In all cases, the quantification of colocalization was represented as Mander's correlation coefficient. 20-30 images per condition were analyzed. Data are shown as mean±SD and analyzed by parametric two-tailed unpaired t-test. Significance was defined as a value of ****p<0.0001.

963

Figure 1

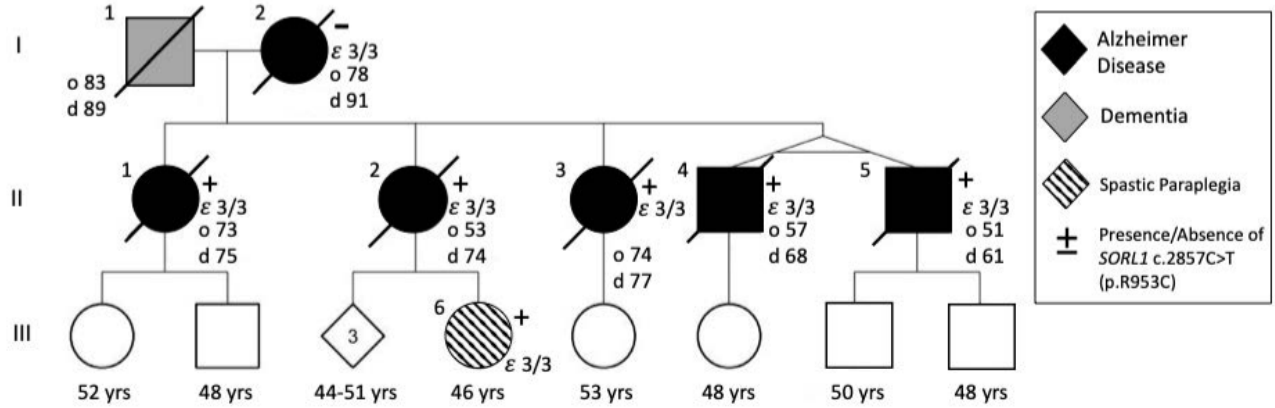

Figure 2

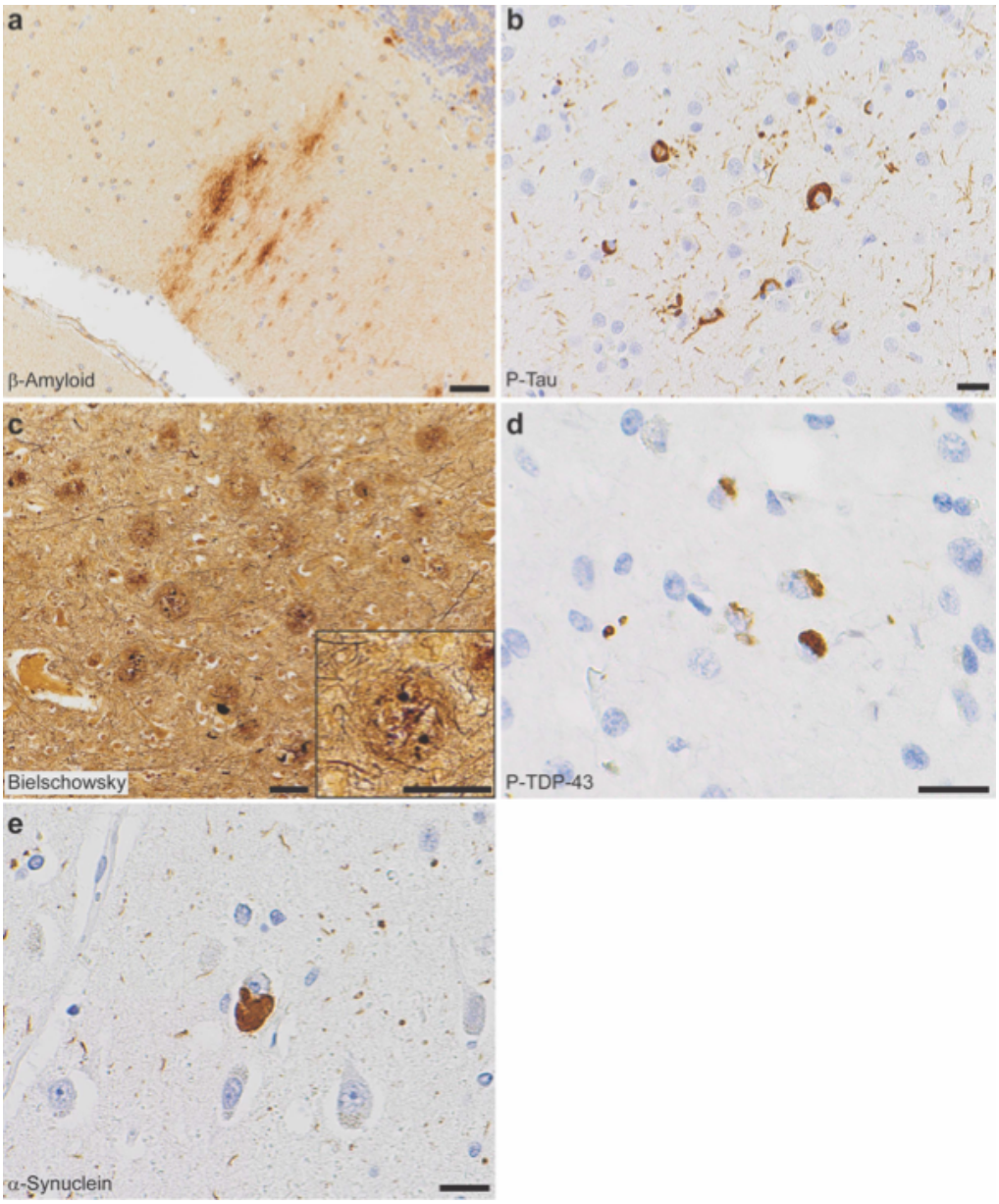

Figure 3

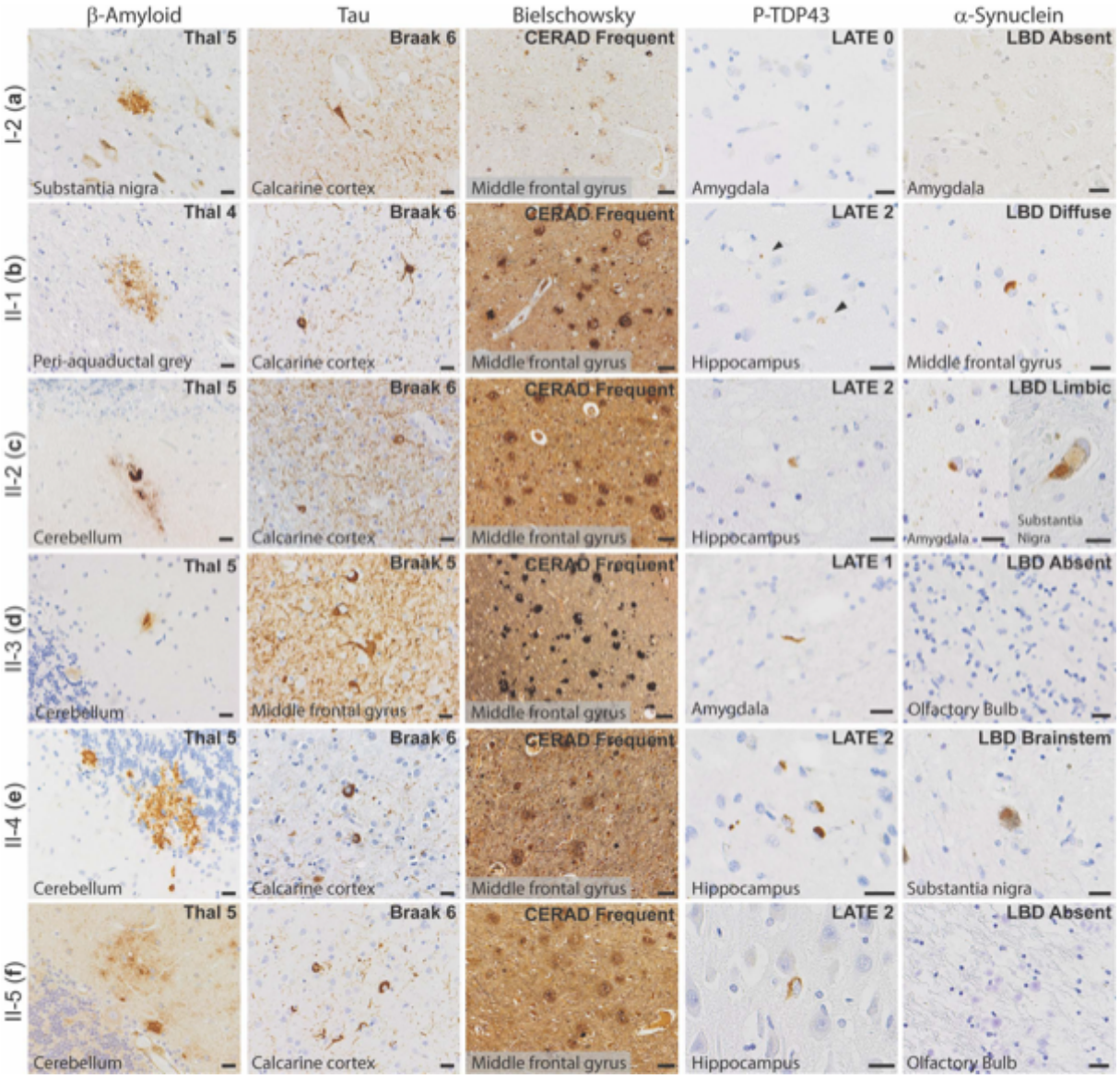

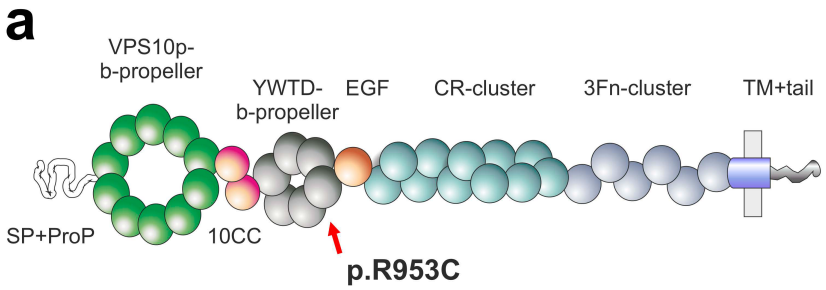

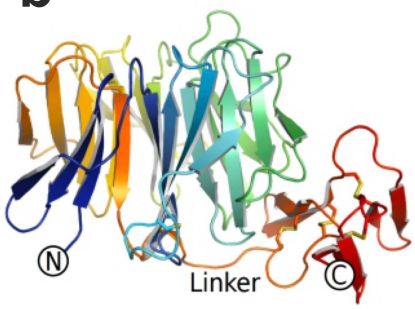

c

```
                    A          B          C          D
                    ----->     ----->     ----->     ----->
                    1         10         20         30         40
β1  754-787     ----------LAEENEFILYAV--RKSIYRYDLASGA--TEQLPL-TGL
β2  788-831     RAAVALDFDYEHNCLYWSDLA--LDVIQRLCL-NGSTGQEVIIN-SGL
β3  832-875     ETVEALAFEPLSQLLYWVDAG--FKKIEVANP-DGDFRLTIVNS-SVL
β4  876-920     DRPRALVLVPQEGVMFWTDWGDLKPGIYRSNM-DGSAAYHLVSE--DV
β5  921-960     KWPNGISVDDQ--WIYWTDAY--LECIERITF-SGQQRSVILD---NL      p.R953C
β6  961-1001    PHPYAIAVFKN--EIYWDDWS--QLSIFRASKYSGS-QMEILAN--QL
β1 1002-1013    TGLMDMKIFYKG----------------------------------
                  P  Φ  Φ      ΦYWTD       I R     G     ΦΦ     L

β5 LDLR         QWPNGITLDLLSGRLYWVDSK--LHSISSIDVNGGN-RKTILEDEKRL     p.R595W
β4 LRP5_2       DEPRAIALHPVMGLMYWTDWG-ENPKIECANL-DGQERRVLVNA--SL     p.R494Q
β3 LRP5_3       DYPEGMAVDWMGKNLYWADTG--TNRIEVARL-DGQFRQVLVWR--DL     p.R752G
β6 LRP5_4       VQPLGLTILGK--HLYWIDRQ--QQMIERVEKTTGDKRTRIQGRVAHL     p.R1188W
β5 LRP4_1       FWPNGLTIDYAGRRMYWVDAK--HHVIERANL-DGSHRKAVISQ--GL     p.R632H
```

d

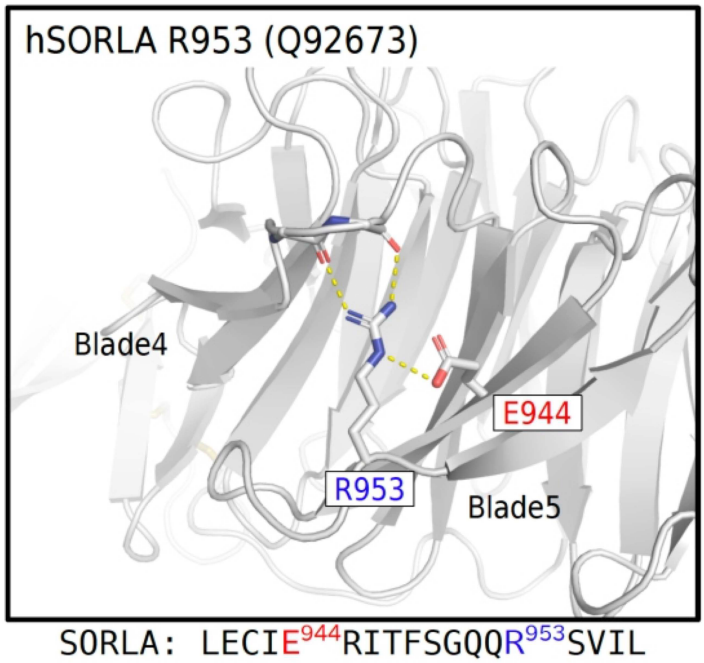

e

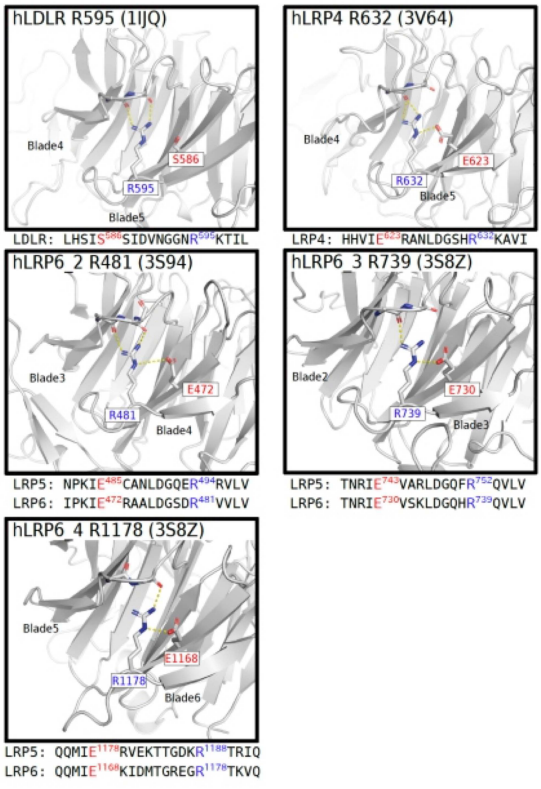

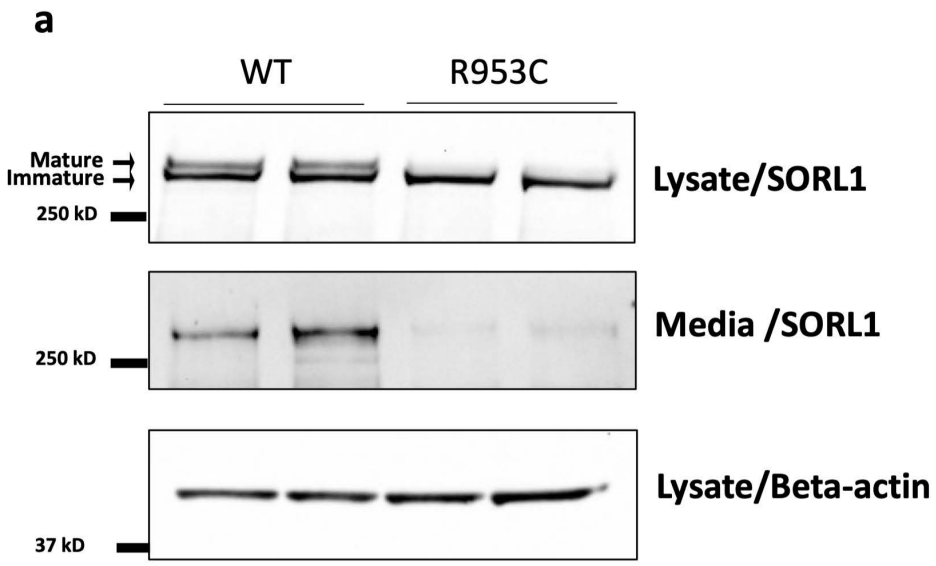

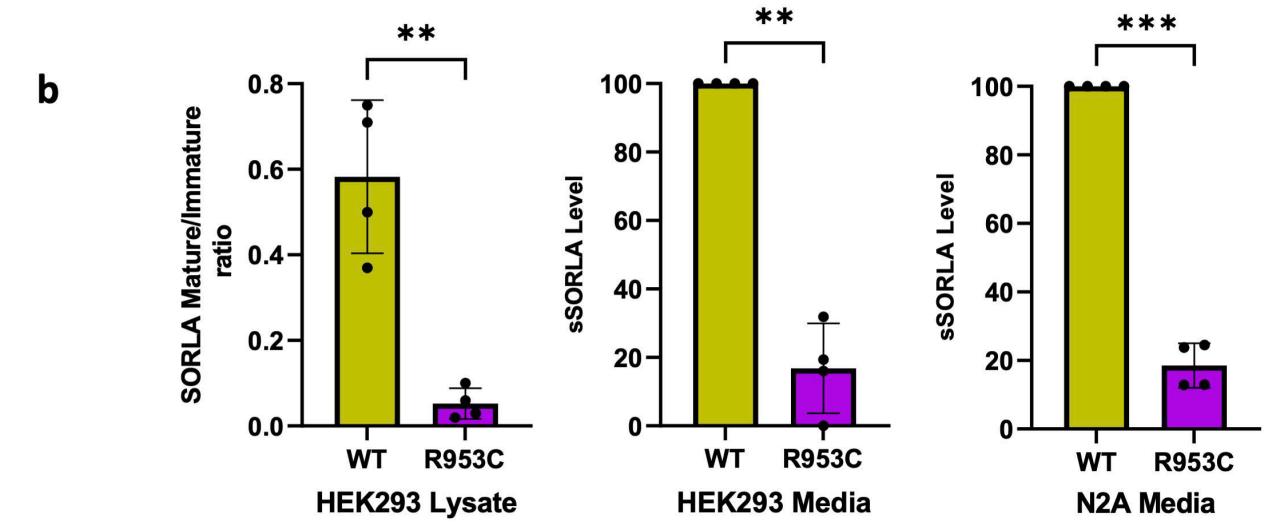

Figure 6

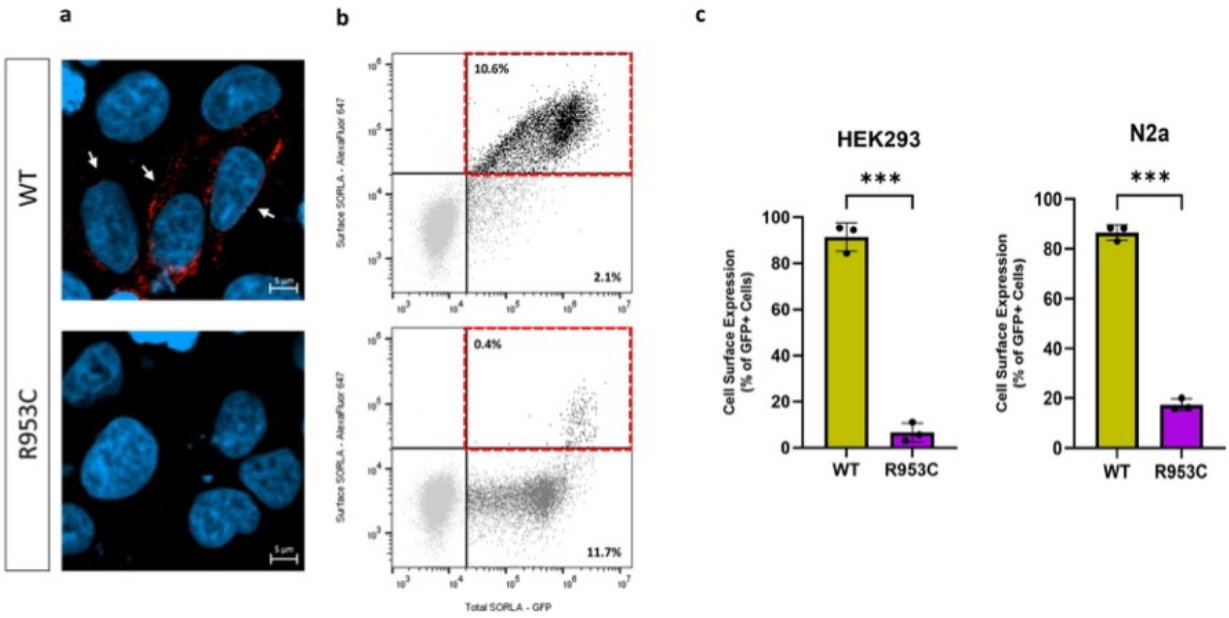

Figure 7

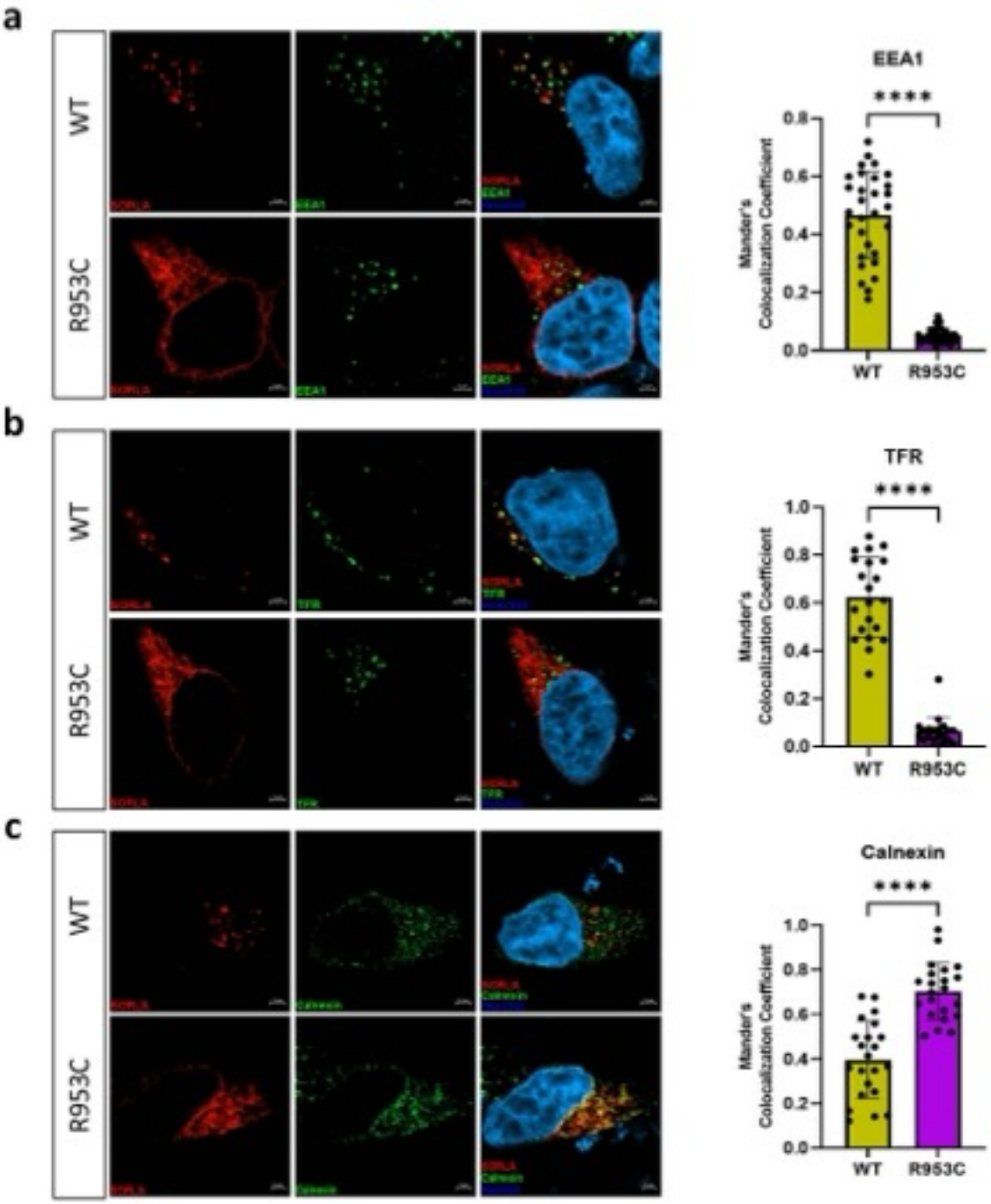

Table 1: Clinical Characterization

Clinical Characterization							
ID	**Sex**	**Age of Onset**	**Age at Death**	**Duration (Years)**	**Clinical Features**	**SORL1 genotype**	**APOE genotype**
I-1	M	83	89	6	Dx "Severe Dementia" Parkinsonism Aggressive Behavior	N/A	N/A
I-2	F	78	91	13	Dx Alzheimer Dementia; Age 85 MMSE 23; Age 86 MMSE 15; Age 87 MMSE 11	WT	**3/3**
II-1	F	73	75	2.5	Dx Alzheimer Dementia; Rapid Progression; Age 74 MOCA 11/30	p.R953C	**3/3**
II-2	F	53	74	21	Dx Alzheimer Dementia; Early Memory Loss in 50's; Age 59 WMS "Profound Impairment"; Age 63 MMSE 26	p.R953C	**3/3**
II-3	F	74	77	3	Dx Alzheimer Dementia; Memory loss, aggression, hallucinations, delusions	p. R953C	**3/3**
II-4	M	57	68	11	Dx Alzheimer Dementia; Age 59 MMSE 26; Twin of II-5	p.R953C	**3/3**
II-5	M	51	61	10	Dx Alzheimer Dementia; Aphasia; Apraxia; Age 55 MMSE 9; Twin of II-4	p.R953C	**3/3**
III-6	F	NA	NA	NA	Dx Spastic paraplegia; Age 45 and Age 46; NP testing - executive dysfunction impaired processing and attention	p.R953C	**3/3**

NP =Neuropsychological Testing

Table 2: Neuropathologic Findings

PEDIGREE NUMBER	BRAIN WEIGHT (G)	ATHERO-SCLEROSIS	THAL PHASE	BRAAK STAGE	CERAD	ADNC	HIPPO-CAMPAL SCELROSIS	LATE STAGE	LEWY BODY DISEASE
I-2	900	Moderate	4	VI	Frequent	HIGH	Absent	0	Absent
II-1	1136	Moderate	4	VI	Frequent	HIGH	Absent	2	Diffuse
II-2	867	Moderate	5	VI	Frequent	HIGH	Present	2	Limbic
II-3	1098	Moderate	5	V	Frequent	HIGH	Absent	1	Absent
II-4	950	Severe	II-4	VI	Frequent	HIGH	Present	2	Brain-stem
II-5	1120	Moderate	5	VI	Frequent	HIGH	Absent	2	Absent

Table 3. Homologous mutations for SORL1 R953C in LDLR and LRP

	Disease	SNP	VarSome	Inheritance pattern	References
p.R595W_LDLR	FH	rs373371572	Pathogenic	A.D.	Descamps et al., 2001 Chiou et al., 2010
p.R494Q_LRP5 p.R494W_LRP5	OPPG FEVR	rs121908664 N.A.	Pathogenic Pathogenic	A.R. A.R.	Gong et al., 2001 Ai et al., 2005 Abdel-Hamid et al., 2022
p.R752G_LRP5 p.R752W_LRP5	FEVR OPPG/FEVR	rs121908674 N.A.	Pathogenic Pathogenic	A.R. A.R.	Jiao et al., 2004 Alonso et al., 2015 Hull et al., 2019
p.R1188W_LRP5	PCLD	rs141178995	Pathogenic	A.D.	Cnossen et al., 2014
p.R632H_LRP4	SOST2	N.A.	Likely Pathogenic	A.R.	Huybrechts et a., 2021

N.A. = Not applicable
A.D. =Autosomal Dominant
A.R. =Autosomal Recessive